

Assessment of celecoxib poly(lactic-co-glycolic) acid nanoformulation on drug pharmacodynamics and pharmacokinetics in rats

S. HARIRFOROOSH¹, K.O. WEST², D.E. MURRELL¹, J.W. DENHAM³,
P.C. PANUS¹, G.A. HANLEY⁴

¹Department of Pharmaceutical Sciences, Gatton College of Pharmacy, East Tennessee State University, Johnson City, TN, USA

²College of Public Health, East Tennessee State University, Johnson City, TN, USA

³Department of Pathology, Quillen College of Medicine, East Tennessee State University, Johnson City, TN, USA

⁴Division of Laboratory Animal Resources, East Tennessee State University, Johnson City, TN, USA

Abstract. – **OBJECTIVE:** Celecoxib (CEL) is a nonsteroidal anti-inflammatory drug (NSAID) showing selective cyclooxygenase-2 inhibition. While effective as a pain reducer, CEL exerts some negative influence on renal and gastrointestinal parameters. This study examined CEL pharmacodynamics and pharmacokinetics following drug reformulation as a poly(lactic-co-glycolic) acid nanoparticle (NP).

MATERIALS AND METHODS: Rats were administered either vehicle (VEH) (methylcellulose solution), blank NP, 40 mg/kg CEL in methylcellulose, or an equivalent NP dose (CEL-NP). Plasma and urine (over 12 hrs) samples were collected prior to and post-treatment. The mean percent change from baseline of urine flow rate along with electrolyte concentrations in plasma and urine were assessed based on 100 g body weight. Using tissues collected 24 hrs post-treatment, gastrointestinal inflammation was estimated through duodenal and gastric prostaglandin E₂ (PGE₂) and duodenal myeloperoxidase (MPO) levels; while kidney tissue was examined for dilatation and necrosis. CEL concentration was assayed in renal tissue and plasma utilizing high-performance liquid chromatography.

RESULTS: Although there were significant changes when comparing CEL and CEL-NP to VEH in plasma sodium concentration and potassium excretion rate, there was no significant variation between CEL and CEL-NP. There was a significant reduction of protective duodenal PGE₂ in CEL compared to VEH ($p = 0.0088$) and CEL-NP ($p = 0.02$). In the CEL-NP formulation, $t_{1/2}$, C_{max} , $AUC_{0-\infty}$, and V_d/F increased significantly when compared to CEL.

CONCLUSIONS: At the observed dosage and duration, CEL-NP may not affect CEL-associated electrolyte parameters in either plasma or urine; however, it does provide increased systemic exposure while potentially alleviating some gastrointestinal outcomes related to inflammation.

Key Words:

NSAIDs, Nanoparticles, Celecoxib, Kidney, Histopathology, Pharmacokinetics.

Introduction

Ranking as one of the most commonly prescribed drug classes the world over, nonsteroidal anti-inflammatory drugs (NSAIDs) provide analgesic, antipyretic, and anti-inflammatory effects to alleviate the symptoms of various ailments in a highly effective manner¹. As the population ages, various ailments which may indicate NSAID usage may also increase; therefore, careful elucidation of NSAID properties is critical to administering these drugs properly and effectively².

Classified on the basis of cyclooxygenase (COX) enzyme selectivity, NSAIDs inhibit prostaglandin production³. One class of NSAIDs is non-selective affecting both COX-1 and COX-2; while another is COX-2-selective. Non-selective NSAIDs may, as a result of non-selectivity, increase the risk of gastric ulcers and intestinal bleeding possibly through the weakening of prostaglandin-dependent mucosal protective mechanisms^{4,5}; likewise, the use of NSAIDs, regardless of class, has been associated with renal

side effects. COX-2-selective inhibitors, such as celecoxib (CEL), can increase kidney dysfunction; however, CEL has displayed minimal gastrointestinal (GI) complications prompting extensive usage³.

Different methods of drug delivery may be used to reduce renal side effects of some drugs. One such method of drug profile alteration is developing a nanoparticle (NP) formulation which may reduce toxicity and side effects^{6,7}. Nanoformulation has also been shown to enhance anti-inflammatory effects and drug retention at the site of action⁸. NP may be constructed of various materials with diverse sizes, shapes, and chemical properties⁹. Polymer-based NP, such as poly(lactic-*co*-glycolic) acid (PLGA) NP, have been used to lessen drug side effects along with enhancing drug bioavailability¹⁰.

In the kidney, PGE₂ plays a regulatory role in fluid metabolism and hemodynamics¹¹. Additional studies have found reduced PGE₂ to have an influential role in the pathogenesis of peptic ulcer disease and damage to the intestines^{5,12,13}. Myeloperoxidase (MPO) is an enzyme located in neutrophils and macrophages; which has been found to be engaged in inflammation and oxidative stress¹⁴. Measuring MPO activity in the intestine can be used to quantitatively to assess inflammation. Thus, PGE₂ and MPO may be used to evaluate inflammation in duodenal and gastric tissue.

The objective of this study is to evaluate nanoformulation of CEL through examination of renal and gastrointestinal outcomes and systemic exposure. A CEL-loaded PLGA nanoparticle (CEL-NP) formulation, developed by our laboratory³, which demonstrates high entrapment efficiency, small particle size, and adequate zeta potential was used for this evaluation.

Materials and Methods

Chemicals

CEL was purchased from Biovision Incorporated (Milpitas, CA, USA). Didodecyldimethylammonium bromide (DMAB), PLGA (50:50 copolymer compositions; MW 20,000-60,000 Da), and ibuprofen were obtained from Sigma-Aldrich (St. Louis, MO, USA); while methylcellulose was bought from Science Stuff Inc. (Austin, TX, USA). High performance liquid chromatography (HPLC)-grade water, glacial acetic acid, iso-octane, 2-propanol, sulfuric acid, triethylamine, ethyl acetate, and acetone were procured from Fischer Scientific Laboratory (Fair Lawn, NJ, USA).

Preparation and Characterization of PLGA-NP Formulation

CEL-NPs were prepared with modifications based on the method previously described by Italia et al¹⁵. Briefly, ethyl acetate (3 mL) was used to dissolve PLGA (50 mg) and CEL (5 mg). The mixture was then stirred (30 min) at room temperature. Following the addition of 6 mL DMAB (0.25% w/v) in a dropwise manner to make an oil-in-water emulsion, the solution was sonicated for 5 minutes at 20 KHz then stirred for 1 hour. The emulsions were centrifuged (18,665 g), then the supernatant was removed. The size (diameter), zeta potential, and polydispersity of the nanoparticles were measured by a NICOMP particle sizer (Particle Sizing Systems, Port Richey, FL, USA). Percent drug entrapment was determined by dividing the amount of drug detected in the nanoparticles, via ultraviolet-visible spectroscopy at 260 nm (Eppendorf Biophotometer, Hauppauge, NY, USA), by the total drug amount used in formulation³.

Animals and Drug Administration

Male Sprague-Dawley rats (*Rattus norvegicus*; Crl:SD; weight, (280-310 g); Charles River Laboratories, Raleigh, NC, USA) were housed in static microisolator cages with aspen bedding (Harlan Teklad, Madison, WI, USA). The animals had a jugular vein catheter placed by the vendor prior to shipping. Rats had unrestricted access to rodent chow (2020X, Harlan Teklad) and water. The room was maintained at standard temperature and humidity (21 ± 2 °C, 30-70%) and on a 12:12 light cycle. Cages were changed once weekly. Serum samples from sentinel animals were tested by multiplex fluorescent immunoassays for coronavirus (sialodacryoadenitis virus/rat coronavirus), rat parvovirus, and rat theilovirus (IDEXX Research ANIMAL Diagnostic Laboratory, Columbia, MO). In addition, rats were free of external and internal parasites. The research protocol was approved by the ETSU University Committee on Animal Care and conducted in AAALAC-accredited facilities.

Study Design

Four groups of rats were examined in this study. The six rats which comprised the methylcellulose (VEH) receiving group were chosen randomly from a pool of 8 identically treated animals. Blank NP were administered to another six rats to provide a negative control for CEL-NP. As previously shown to significantly alter electrolyte excretion, a 40 mg/kg dose of CEL was selected for this study¹⁶. Thus CEL, dissolved in a 0.5% methylcellulose solution,

was given to another group (n = 6). Finally, six rats were treated with a 40 mg/kg CEL dose equivalent amount of CEL-NP suspension. All treatments were administered via a stainless steel straight feeding needle (18 ga, 3 inches).

Immediately after dosing, the animals were housed in metabolic cages (Lab Products Inc., Seaford, DE, USA) to obtain urine samples (12 hrs). Twenty-four hours following treatment, the rats were deeply anesthetized using isoflurane and exsanguinated via cardiac puncture. A portion of the small intestine (duodenum, proximal 8 cm, sectioned longitudinally) and the stomach was collected and washed in 0.9% normal saline and blot dried. The dried samples were then homogenized, using a PowerGen 700 homogenizer (Fisher Scientific, Pittsburgh, PA, USA), and used for determination of PGE₂ and/or MPO levels. Kidneys were also collected and stored at -80 °C. Kidney samples were also homogenized (a 2:1 ratio of milliliters water to milligrams sample) when used for CEL concentration assay.

Renal Function Parameters

Change in Urine Flow Rate

The mean percent change of urine flow rate was assessed by dividing the total urine volume (mL) collected each day (baseline and following treatment) by the duration (12 hrs) of collection and normalized based on respective body weights (100 g B.W.).

Change in Urinary and Plasma Electrolytes

An EasyLyte analyzer (Medica Corporation, Bedford, MA, USA) was utilized to establish sodium and potassium levels (mM) in urine and plasma collected at baseline and following treatment. An equation, $C \times V \times 100/T \times W$, was used to calculate urinary sodium and potassium excretion rates. C representing the respective electrolyte concentration in the urine sample, V as the total urine volume in milliliters, T being the duration of urine collection (12 hrs), and W as body weight (100 g). Parameters were then converted to mean percent change from baseline.

Kidney Histopathological Assessment

A section of rat kidney was collected following partial thaw; fixed in formalin overnight; then embedded in paraffin wax for sectioning. Sections of the kidney were obtained at 5 μm then

stained with hematoxylin and eosin. All sections were examined and graded for two parameters on a scale ranging from 0 to 3 (normal, mild, moderate, or severe tubular dilatation and 0, 10, 10-25, or >25% necrosis) by a board certified pathologist blinded to the treatment groups.

Gastrointestinal Inflammatory Factors

Gastric and Intestinal PGE₂

PGE₂ levels were determined by an enzyme-linked immunosorbent assay (ELISA) (Antibodies-Online Inc., Atlanta, GA, USA). Utilizing a sample of gastric or intestinal tissue, the ELISA was performed according to the manufacturer's instructions. The optical density (OD at 450 nm) was positively correlated with the amount of PGE₂ present within the sample. MyAssays software (MyAssays Ltd, Sussex, UK) was used to determine concentrations.

Intestinal MPO

MPO levels were also measured via an ELISA kit (Kamiya Biomedical Company, Seattle, WA, USA). The quantity of MPO was examined using guidelines provided by the manufacturer. The technique utilized a quantitative sandwich enzyme immunoassay with a microtiter plate pre-coated with MPO-specific antibodies. Biotin-conjugated MPO was added to standards and samples then avidin-conjugated HRP was introduced following a wash. The substrate solution was added after an additional wash followed by a color change. This was measured at a wavelength of 450 nm with correction at 540 nm. Sample concentrations were determined using MyAssays software.

Chromatographic Conditions

Analysis Equipment and Solution Preparation

A Shimadzu HPLC (Shimadzu Scientific Instruments Inc., Columbia, MD, USA) equipped with a DGU-20A Prominence degasser, a SIL-20A HT auto sampler, a CBM-20A communication bus module, a SPD-M20A diode array detector (254 nm), a LC020AB solvent delivery system, and a CTO-20A column oven with a Phenomenex C18 column (100 × 4.6 nm; 2.6 μm; Torrance, CA, USA) installed was used for drug concentration analysis.

CEL concentration was assayed by a previously described method with modifications based on sample type¹⁶. Stock solutions (100,000 ng/mL) of CEL and ibuprofen, the internal standard

(IS), were added to blank plasma or kidney homogenate (100 μ L). Two hundred microliters of 0.6 M sulfuric acid along with five milliliters of 95:5 iso-octane isopropanol was added to each sample then vortex mixed (30 s). Following centrifugation (5 minutes at 2,500 g), samples were placed in a dry ice/ethanol bath to facilitate organic phase removal. Set at 50 °C, sample organic phases were evaporated prior to reconstitution in a CentriVap Concentrator (Lab Conoco, Kansas City, MO, USA). Samples were reconstituted in mobile phase (200 μ l) then 100 μ l injected. The mobile phase consisted of acetonitrile-water-acetic acid-triethylamine (47:53:0.1:0.03) ran at a flow rate of 1 mL/min. The plasma assay gave a lower limit of quantitation (LLQ) at 250 ng/mL to have a coefficient of variation (CV) of 3% while providing a lower limit of detection (LLD) of 100 ng/mL; while the kidney assay provided a LLD of 100 ng/g and a LLQ of 250 ng/g with a CV of 3.7%.

Pharmacokinetic Analysis

Pharmacokinetic serial blood sampling consisted of 9 time points (0, 0.5, 1, 2, 4, 6, 8, 12, and 24 hrs). A non-compartment component of Phoenix WinNonlin 6.3 (Certara USA, Inc., Princeton, NJ, USA) was utilized to determine various pharmacokinetic parameters based on plasma concentration, maximum plasma concentration (C_{max}), half-life ($t_{1/2}$), area under the plasma concentration-time curve from time zero to infinity ($AUC_{0-\infty}$), apparent oral clearance (CL_{oral}), and apparent volume of distribution (Vd/F). CEL kidney distribution was also assayed.

Data Treatment and Statistical Analysis

For urine flow rate and electrolyte concentrations and excretion rates, mean percent change was calculated from baseline and post-treatment values using the following formula: $((\text{Post-treatment} - \text{baseline})/\text{baseline}) \times 100$. Urinary values, along with PGE_2 and MPO levels, were calculated for each measure and compared using one-way ANOVA following the PROC GLM procedure in SAS (SAS Institute Inc., Cary, NC, USA). Individual drug plasma concentrations, along with all non-histological values, were examined for outliers using IBM SPSS Statistics software version 21 (Armonk, NY, USA). Those rats, for which the elimination phase was unavailable, were removed from pharmacokinetic consideration. Pharmacokinetic comparisons were made between CEL and CEL-NP by a Student's t-test. Statistical sig-

nificance was set at $p < 0.05$. Values are presented as mean \pm standard error of the mean.

For histologic scores, Kruskal-Wallis one-way analysis was performed. Pairwise comparisons were made between groups using a post hoc test for minimal significant difference between groups¹⁷. Calculated difference between the mean-of-ranks for the two groups was compared to tabulated value for familywise error rate with a significance set at 0.05 and adjusted for sample size. A total of 5 comparisons were made with "z" set at 2.576. For the renal dilation histology, one outlier from each group, VEH and CEL-NP, was removed prior to calculations. No groups were removed from renal tubular necrosis histology assessment.

Results

Characteristics of Celecoxib-Loaded PLGA-NPs

The CEL-NP ($n = 3$) used in this study were determined to have a diameter of 79.13 ± 0.69 nm and a mean zeta potential of 21.37 ± 0.25 mV with a polydispersity of 0.17 ± 0.02 . Drug entrapment efficiency was $86.28 \pm 0.08\%$.

Renal Function Assessments

Change in Urine Flow Rate

ANOVA testing of mean percent change (Figure 1) showed no significant changes among treatment groups ($p = 0.0834$).

Change in Urinary Electrolytes

While the mean percent change in sodium excretion rates shown in Figure 2 presented with no significant difference among groups ($p = 0.1648$), the mean percent change in potassium excretion rates (Figure 3) differed significantly within groups ($p = 0.0012$). Groups receiving NP ($-16.62 \pm 9.27\%$; $p = 0.0034$), CEL ($-26.15 \pm 5.57\%$; $p = 0.0006$), or CEL-NP ($-31.54 \pm 13.46\%$; $p = 0.0004$) each displayed a significant mean percent decrease when compared to VEH ($23.56 \pm 5.02\%$).

Change in Plasma Electrolytes

A significant difference was detected among groups in regard to mean percent change in plasma sodium concentration ($p = 0.0018$). The mean percent change increase in plasma sodium concentration (Figure 4) was significantly reduced

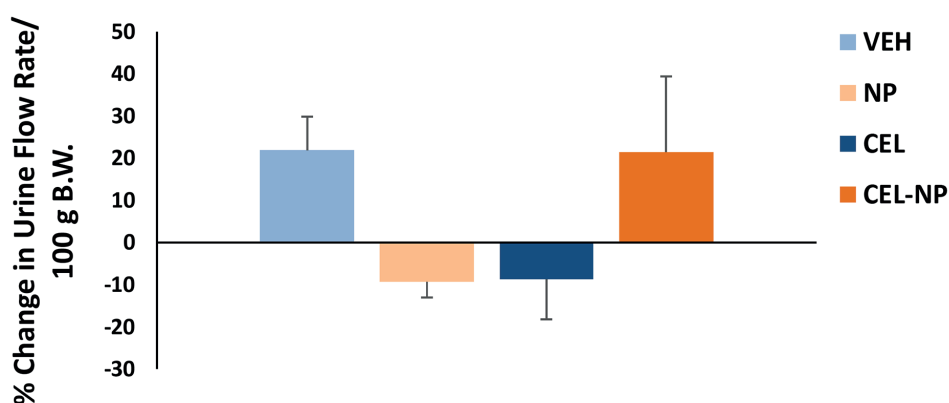


Figure 1. Mean Percent Change in Urine Flow Rate. Mean percent change from baseline of urine flow rate in groups treated with vehicle (VEH; $n = 6$), nanoparticles (NP; $n = 6$), celecoxib (CEL; $n = 5$), or celecoxib-loaded nanoparticles (CEL-NP; $n = 6$). The values are expressed as percent change \pm standard error of the mean. The values were not significantly different, $p \geq 0.05$.

when comparing CEL ($3.80 \pm 1.40\%$; $p = 0.0002$) and CEL-NP ($8.17 \pm 1.46\%$; $p = 0.0402$) to VEH ($12.13 \pm 0.85\%$). There was no significant difference between NP and VEH ($p = 0.0972$). Evaluations of plasma potassium concentration mean percent changes (Figure 5) showed no statistical significance among groups.

Histopathological Assessments

Upon histopathological examination, as displayed in Figure 6-A, the VEH group showed mild dilatation in every kidney; while necrosis was not seen in the VEH group. The NP group (Figure 6-B) also showed mild to moderate dilatation and varying levels of necrosis from none to moderate. In Figure 6-C, sections from the

CEL group showed tubular dilatation ranging from mild to moderate (1-2) with no necrosis. The CEL-NP group (Figure 6-D) showed moderate dilatation in all but one kidney, which had mild dilatation with necrosis ranging from none to mild. Overall, no statistical significance for tubular dilatation or necrosis was observed among the groups.

Histological scoring of each group along with mean-rank is presented in Table I. Statistical analysis of the renal histology demonstrated no significant difference, tie-adjusted H score 6.65 ($k = 4$, tabulated = 7.82), between the treatment groups for renal dilatation. In contrast, the tie-adjusted H score of 8.75 was significant for renal necrosis histology ($k = 4$, tabulated = 7.82). For

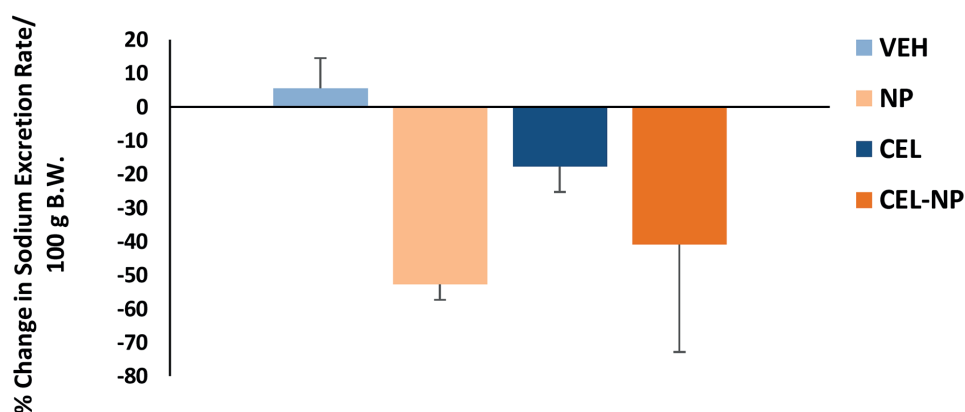


Figure 2. Mean Percent Change in Sodium Excretion Rate. Mean percent change from baseline of sodium excretion rates in groups treated with vehicle (VEH; $n = 4$), nanoparticles (NP; $n = 5$), celecoxib (CEL; $n = 5$), or celecoxib-loaded nanoparticles (CEL-NP; $n = 5$). The values are expressed as percent change \pm standard error of the mean. The values were not significantly different, $p \geq 0.05$.

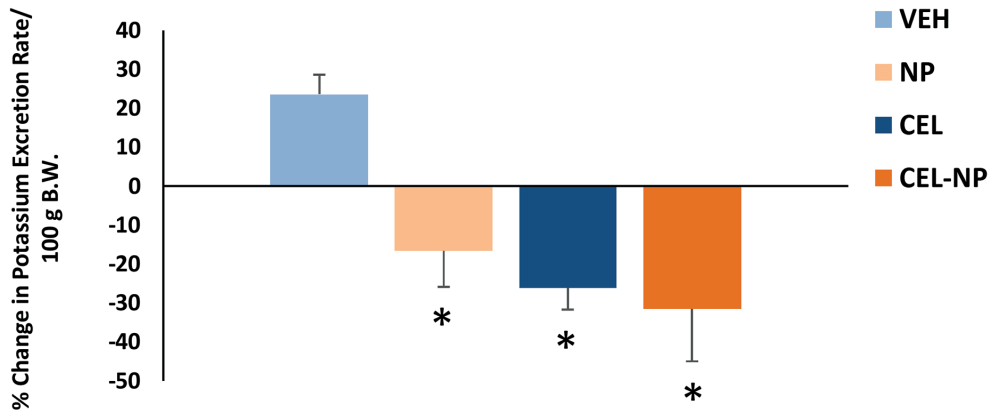


Figure 3. Mean Percent Change in Potassium Excretion Rate. Mean percent change from baseline of potassium excretion rates in groups treated with vehicle (VEH; n = 5), nanoparticles (NP; n = 5), celecoxib (CEL; n = 5), or celecoxib-loaded nanoparticles (CEL-NP; n = 4). The values are expressed as percent change \pm standard error of the mean. * $p < 0.05$, significantly different from VEH.

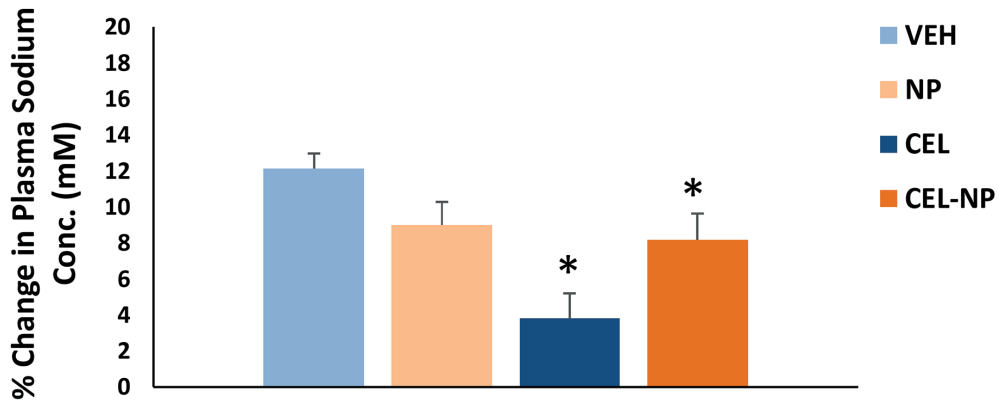


Figure 4. Mean Percent Change in Plasma Sodium Concentration. Mean percent change from baseline of plasma sodium concentration in groups treated with vehicle (VEH; n = 6), nanoparticles (NP; n = 6), celecoxib (CEL; n = 6), or celecoxib-loaded nanoparticles (CEL-NP; n = 6). The values are expressed as percent change \pm standard error. * $p < 0.05$, significantly different from VEH.

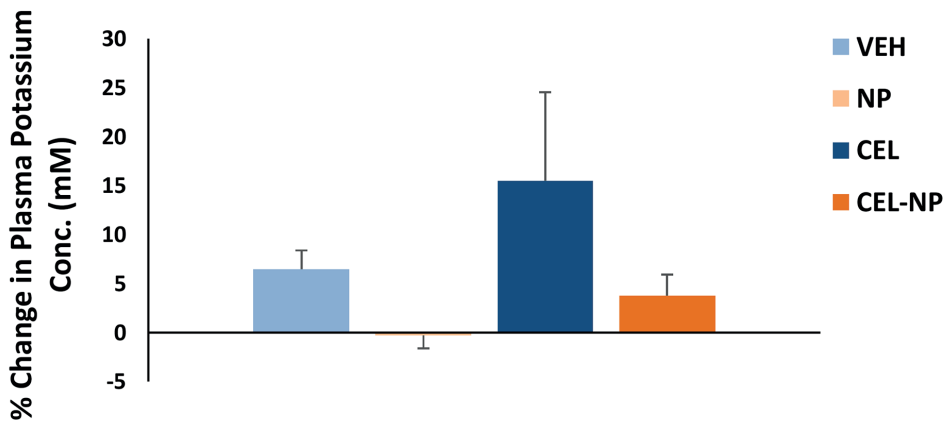


Figure 5. Mean Percent Change in Plasma Potassium Concentration. Mean percent change from baseline of plasma potassium concentration in groups treated with vehicle (VEH; n = 6), nanoparticles (NP; n = 5), celecoxib (CEL; n = 5), or celecoxib-loaded nanoparticles (CEL-NP; n = 6). The values are expressed as percent change \pm standard error of the mean. The values were not significantly different, $p \geq 0.05$.

Table I. Histopathological assessment of tubular dilatation and necrosis.

Group	Tubular Dilatation Scores						Tubular Necrosis Scores					
	0	1	2	3	n	Mean-Rank	0	1	2	3	n	Mean-Rank
VEH	0	5	0	0	5	7.0	6	0	0	0	6	9.5
NP	0	4	2	0	6	10.7	4	1	1	0	6	13.8
CEL	0	3	3	0	6	12.5	6	0	0	0	6	9.5
CEL-NP	0	1	4	0	5	15.8	2	4	0	0	6	17.2

Tubular dilatation and necrosis scores in the groups treated with methylcellulose (VEH), empty nanoparticles (NP), celecoxib (CEL), celecoxib-loaded nanoparticles (CEL-NP).

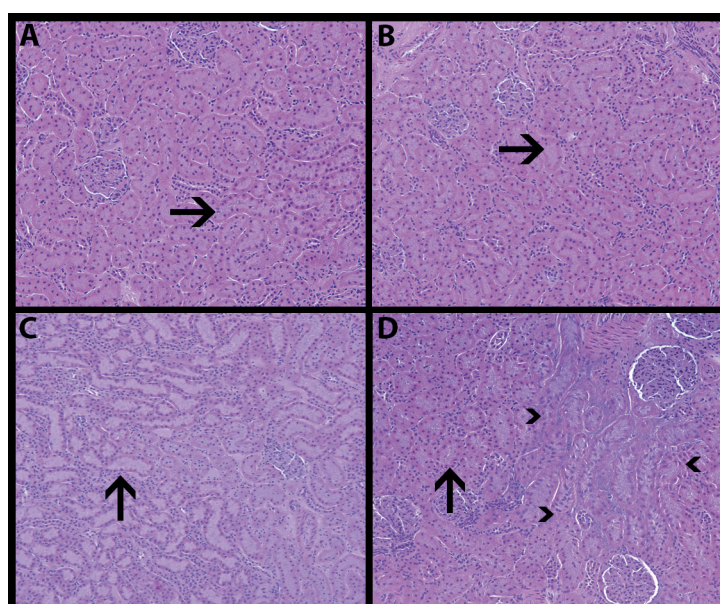


Figure 6. Kidney Histopathology. Kidney cross sections (hematoxylin & eosin stained) from rat groups treated with A (vehicle) and B (blank nanoparticles) showing mild tubular dilatation (arrow) and no areas of necrosis. C (celecoxib) showed moderate tubular dilatation (arrow) and no areas of necrosis; while D (celecoxib-loaded nanoparticles) presented with moderate tubular dilatation (arrow) with mild necrosis (arrow heads). 20× magnification.

the five post hoc two group comparisons examined the VEH group demonstrated no significant differences to the NP, CEL, or CEL-NP group. Additionally, no differences were observed in the comparison of the CEL group to the CEL-NP group, or NP group to the CEL-NP group.

Gastrointestinal Inflammatory Factors

When each treatment group was compared, there was no significant increase in PGE₂ levels (Figure 7) in gastric tissue ($p = 0.6151$). In contrast, as shown in Figure 8, significant difference was detected ($p = 0.0367$) in duodenal PGE₂ concentration. PGE₂ levels in the intestine did not differ significantly between NP vs VEH ($p = 0.1419$) and CEL-NP vs VEH ($p = 0.6229$); however, there was a significant decrease in CEL (68.97 ± 7.94 pg/mL) when compared to VEH (94.27 ± 3.60 pg/mL; $p = 0.0088$) and CEL-NP (89.94 ± 3.24 pg/mL; $p = 0.0200$). When intestinal MPO was examined among

treatment groups, no significant differences were found ($p = 0.2767$; Figure 9).

Pharmacokinetics of Celecoxib

As shown in Figure 10, no significance difference ($p = 0.5424$) was detected in renal CEL concentration between formulations. The plasma concentration time curve from each formulation is given in Figure 11, while pharmacokinetic parameters are presented in Table II. C_{\max} ($p = 0.0017$), $AUC_{0-\infty}$ ($p = 0.0158$), $t_{1/2}$ ($p = 0.0203$), and Vd/F ($p = 0.0056$) were significantly increased in the CEL-NP formulation compared to CEL. CL_{oral} ($p = 0.0714$) was not significantly changed between formulations.

Discussion

NSAIDs are often used to reduce pain and inflammation associated with arthritis²; however, NSAIDs have both beneficial and detri-

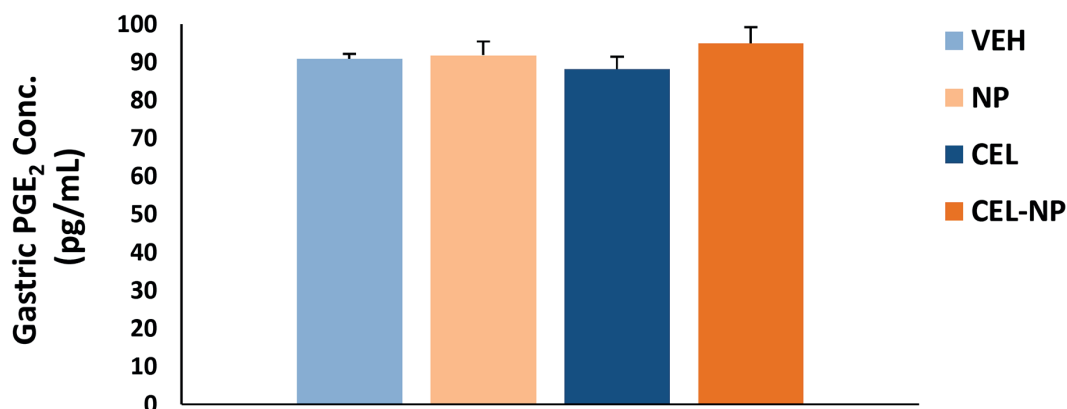


Figure 7. Gastric PGE₂ Concentration. Effect of treatment with vehicle (VEH; n = 3), nanoparticles (NP; n = 6), celecoxib (CEL; n = 6), or celecoxib-loaded nanoparticles (CEL-NP; n = 6) on gastric PGE₂ concentration. The values are expressed as mean ± standard error of the mean. The values were not significantly different, $p \geq 0.05$.

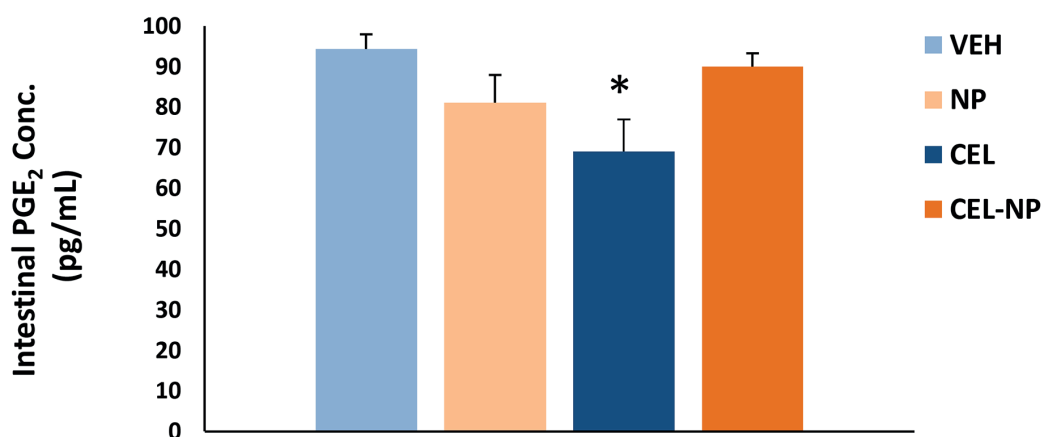


Figure 8. Intestinal PGE₂ Concentration. Effect of treatment with vehicle (VEH; n = 5), nanoparticles (NP; n = 6), celecoxib (CEL; n = 6), or celecoxib-loaded nanoparticles (CEL-NP; n = 6) on intestinal PGE₂ concentration. The values are expressed as mean ± standard error of the mean. * $p < 0.05$, significantly different from VEH.

mental effects. Using a NP-based formulation, negative side-effects may be minimized⁶. The objective of this study was to compare renal and gastrointestinal effects of CEL in a PLGA-NP formulation and to evaluate the pharmacokinetic profile of the formulation.

Signs of kidney damage may include reduced urine outflow and electrolyte excretion¹⁸. Previous studies in rats have shown that CEL can produce negative kidney side effects relative to reduced excretion of electrolytes even when measured urine flow rate was unchanged. In this stu-

Table II. The pharmacokinetic parameters of celecoxib following a single oral dose of celecoxib (40 mg/kg) or a PLGA nanoparticle equivalent.

Formulation	n	$t_{1/2}$ (hr)	C_{max} ($\mu\text{g/mL}$)	$AUC_{0-\infty}$ ($\mu\text{g}\cdot\text{h/mL}$)	Cl_{oral} (L/h/kg)	V_d/F (L/kg)
CEL	5	10.22 ± 1.11	1.71 ± 0.18	32.25 ± 3.50	1.32 ± 0.18	18.92 ± 2.46
CEL-NP	4	5.99 ± 0.73*	2.86 ± 0.13*	45.11 ± 1.00*	0.89 ± 0.02	7.62 ± 0.77*

CEL-celecoxib; CEL-NP-celecoxib-loaded nanoparticles. Values expressed as mean ± standard error of the mean. * $p < 0.05$, significantly different from CEL.

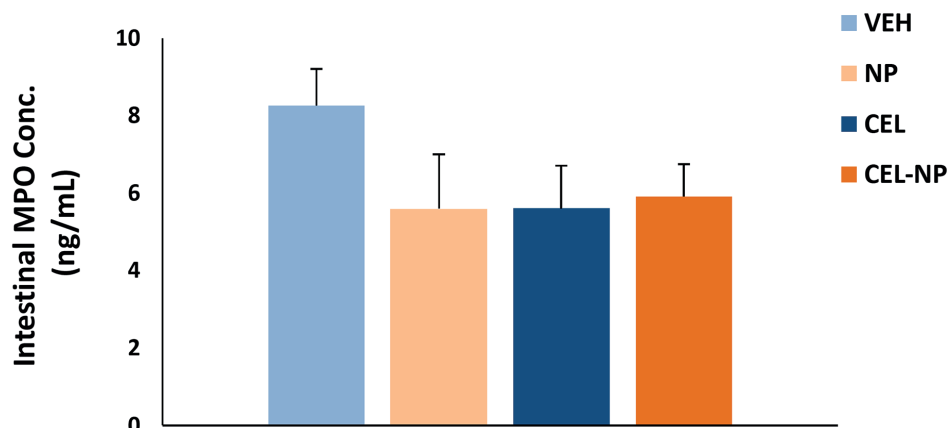


Figure 9. Intestinal MPO Concentration. Effect of treatment with vehicle (VEH; $n = 6$), nanoparticles (NP; $n = 6$), celecoxib (CEL; $n = 6$), or celecoxib-loaded nanoparticles (CEL-NP; $n = 6$) on intestinal MPO concentration. The values are expressed as mean \pm standard error of the mean. The values were not significantly different, $p \geq 0.05$.

dy, we examined the effect of nanoformulation on CEL generated renal damage by comparing urine flow rate and electrolyte excretion rate among treatment groups. The urine flow rate results found in our study agree with previous findings in that neither CEL nor CEL-NP demonstrated significant change compared to VEH (Figure 1). In Figure 2, sodium excretion rate among groups was not found to be significantly different perhaps due to high variation within the CEL-NP group. Although potassium excretion rate showed a variation when comparing groups to VEH, there was no notable difference between CEL and CEL-NP (Figure 3). A significant decrease in plasma sodium concentration was seen among the treatment groups with no significant change in plasma potassium (Figures 4 and 5). These results may be limited by high variation within those groups which did not show significance.

Physical changes produced by drug administration were seen in the renal histopathological analysis; however, there was no statistical variation among groups for tubular dilatation or necrosis (Figure 6). Another investigation¹⁹ has reported that CEL produces tubular degeneration at 50 mg/kg. In our study, the dosage and time of observation after drug administration was only one day, compared to 28 days in the study performed by Koçkaya et al¹⁹. Thus limited treatment duration may explain our result. Results similar to the present study, in terms of no significant change in liver histopathology, have been observed previously following either 24 hours or 7 days of exposure to CEL (40 mg/kg)^{20,21}.

Gastric PGE₂ levels did not show any significant variation among groups (Figure 7). In previous studies, gastric PGE₂ levels were not affected by CEL (5 mg/kg) in rats without previous ulcers²². Although our dose was higher, this correlates with our findings. There was a significant decrease of intestinal PGE₂ in CEL when compared to VEH as seen in Figure 8. This could increase inflammation, ulcers, and other adverse effects associated with decreased PGE₂. A previous research²³ in mice, showed that 3 hours following a single dose (300 mg/kg) of CEL intestinal PGE₂ levels were not altered. Our results at 24 hours at 40 mg/kg showed a change, but did not present with significance. In agreement with our MPO results (Figure 9), Demircan et al¹⁸ found MPO levels to be lowest following CEL dosing when comparing indomethacin, meloxicam, and CEL. CEL-NP showed similar results to VEH which may indicate a decreased risk of gastrointestinal side effects and inflammation that have been associated with CEL.

CEL-NP showed no significant difference in renal CEL concentration when compared to CEL (Figure 10). In Figure 11 and Table II, C_{max} and $AUC_{0-\infty}$ were significantly increased in the CEL-NP formulation compared to CEL. This relates to a higher systemic exposure and an increased bioavailability for CEL-NP compared to CEL. Enhanced bioavailability of CEL-NP is supported by results seen in a formulation of CEL-PVP-TPGS solid dispersion nanoparticles through which Ha et al²⁴ significantly increased the oral absorption of CEL. Similar results were also found by Morgen et al²⁵ further establishing that NP are sufficient for delivering enhanced bioavailability of

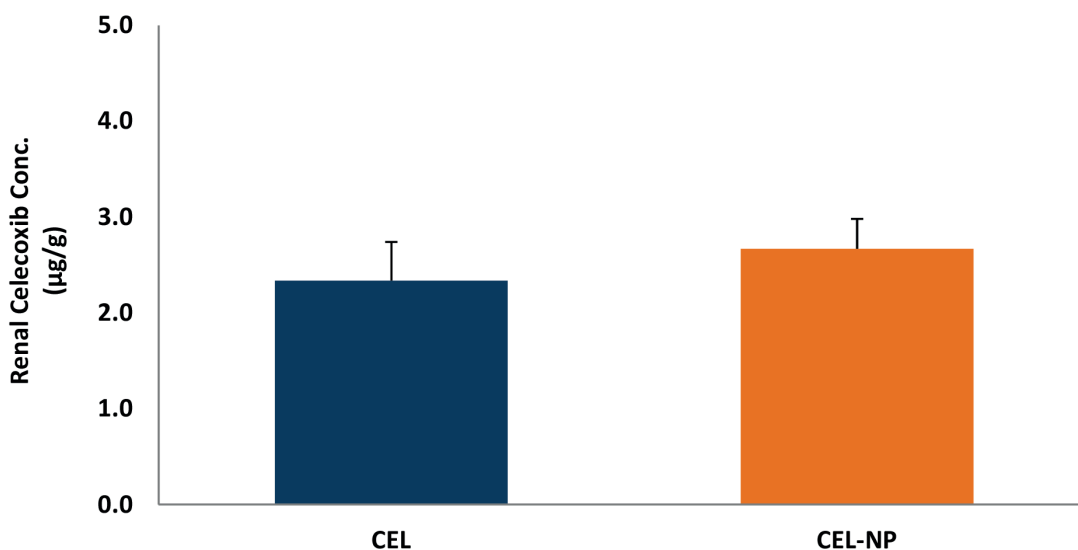


Figure 10. Renal Celecoxib Concentration. Renal concentration of celecoxib following a single 40 mg/kg oral dose of celecoxib (CEL; n = 5) or a celecoxib-loaded nanoparticle (CEL-NP; n = 4) equivalent. The values are expressed as mean ± standard error of the mean. The values were not significantly different, $p \geq 0.05$.

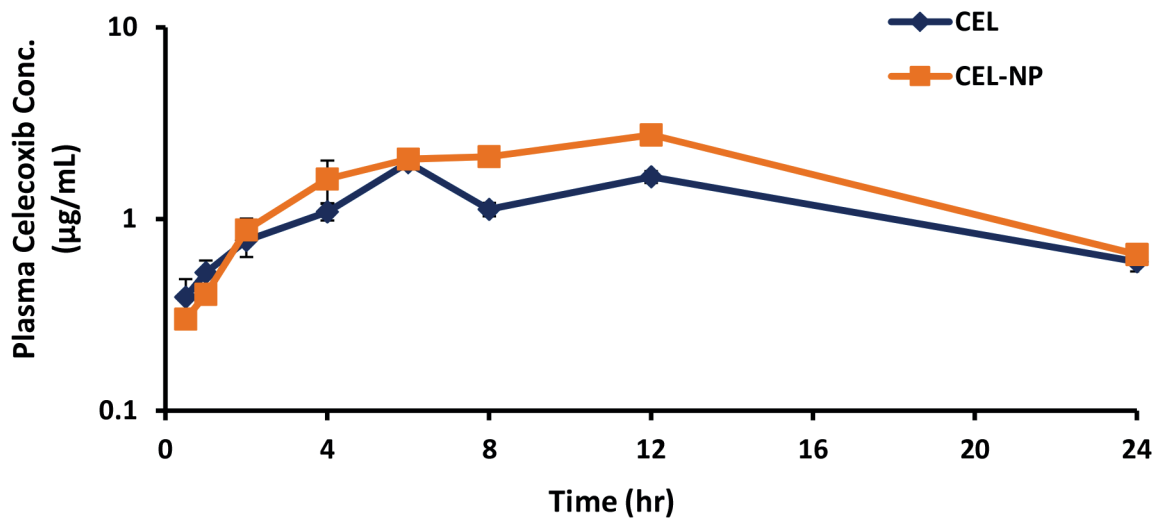


Figure 11. Celecoxib Plasma Concentration-time Curve. Plasma concentration-time profile of celecoxib following a single 40 mg/kg oral dose of celecoxib (CEL; n = 5) or a celecoxib-loaded nanoparticle (CEL-NP; n = 4) equivalent. The values are expressed as mean ± standard error of the mean.

Biopharmaceutics Classification System Class II drugs, like CEL. Although the systemic exposure was increased in our study, there was no accumulation in the kidney.

Several characteristics of this work may be limitations. While observing the renal and gastrointestinal side effects of CEL, we only used a single dose of 40 mg/kg. While this dosage found significant results related to levels of PGE₂ compared to VEH and also enhanced bioavailability, these asso-

ciations may not be representative of a wide range of CEL or CEL-NP usage because they were made using a single dose. The action of CEL has been extensively studied in relation to gastrointestinal and renal side effects; however, the proposed NP formulations of the NSAID and their associated side effects have not been comprehensively studied. NP are a developing technology and given the diverse formulations and compounds; it is challenging to compare those results to our study.

Conclusions

This report indicates that this CEL-NP did not alter kidney histopathology or renal CEL concentration at the treatment dose and duration examined; however, PLGA-nanoformulation significantly enhanced systemic exposure. Although potentially helping to stabilize the change in PGE₂ in intestinal tissue of rats, the NP formulation may not influence electrolyte parameters in plasma and urine. Overall, our results support a promising NP delivery system for increasing systemic exposure of the poorly water-soluble drug, CEL.

Acknowledgements

We would like to thank Dustin Cooper, Angela Hanley, and Kenny Bullins for their technical assistance.

Funding

This study was funded by a grant from the East Tennessee State University Research Development Committee Major Grants Program. This research was supported in part by the National Institutes of Health grant C06RR0306551.

Conflicts of interest

The authors declare no conflicts of interest.

References

- 1) GAN TJ. Diclofenac: an update on its mechanism of action and safety profile. *Curr Med Res Opin* 2010; 26: 1715-1731.
- 2) CROFFORD LJ. Use of NSAIDs in treating patients with arthritis. *Arthritis Res Ther* 2013; 15 Suppl 3: S2.
- 3) COOPER DL, HARIRFOROOSH S. Effect of formulation variables on preparation of celecoxib loaded polylactide-co-glycolide nanoparticles. *PLoS One* 2014; 9: e113558.
- 4) TAKEUCHI K, TANAKA A, KATO S, AMAGASE K, SATOH H. Roles of COX inhibition in pathogenesis of NSAID-induced small intestinal damage. *Clin Chim Acta* 2010; 411: 459-466.
- 5) PARK SM, YOO BC, LEE HR, CHUNG H, LEE YS. Distribution of prostaglandin E2 in gastric and duodenal mucosa: possible role in the pathogenesis of peptic ulcer. *Korean J Intern Med* 1992; 7: 1-8.
- 6) DE JONG WH, BORM PJ. Drug delivery and nanoparticles: applications and hazards. *Int J Nanomedicine* 2008; 3: 133-149.
- 7) COOPER DL, CARMICAL JA, PANUS PC, HARIRFOROOSH S. Formulation and *in vitro* evaluation of niacin-loaded nanoparticles to reduce prostaglandin mediated vasodilatory flushing. *Eur Rev Med Pharmacol Sci* 2015; 19: 3977-3988.
- 8) SHAKEEL F, BABOOTA S, AHUJA A, ALI J, SHAFIO S. Enhanced anti-inflammatory effects of celecoxib from a transdermally applied nanoemulsion. *Pharmazie* 2009; 64: 258-259.
- 9) MUDSHINGE SR, DEORE AB, PATIL S, BHALGAT CM. Nanoparticles: emerging carriers for drug delivery. *Saudi Pharm J* 2011; 19:129-141.
- 10) PARHI P, MOHANTY C, SAHOO SK. Nanotechnology-based combinational drug delivery: an emerging approach for cancer therapy. *Drug Discov Today* 2012; 17:1044-1052.
- 11) JIA Z, ZHANG Y, DING G, HEINEY KM, HUANG S, AND ZHANG A. Role of COX-2/mPGES-1/prostaglandin E2 cascade in kidney injury. *Mediators Inflamm*. 2015: 147894. 2015.
- 12) ONG CK, LIRK P, TAN CH, SEYMOUR RA. An evidence-based update on nonsteroidal anti-inflammatory drugs. *Clin Med Res* 2007; 5: 19-34.
- 13) MONTROSE DC, NAKANISHI M, MURPHY RC, ZARINI S, McALEER JP, VELLA AT, ROSENBERG DW. The role of PGE₂ in intestinal inflammation and tumorigenesis. *Prostaglandins Other Lipid Mediat* 2015; 116-117:26-36.
- 14) LORIA V, DATO I, GRAZIANI F, BIASUCCI LM. Myeloperoxidase: a new biomarker of inflammation in ischemic heart disease and acute coronary syndromes. *Mediators Inflamm* 2008; 2008: 135625.
- 15) ITALIA JL, BHATT DK, BHARDWAJ V, TIKOO K, KUMAR MN. PLGA nanoparticles for oral delivery of cyclosporine: nephrotoxicity and pharmacokinetic studies in comparison to Sandimmune Neoral. *J Control Release* 2007; 119: 197-206.
- 16) HARIRFOROOSH S, AGHAZADEH-HABASHI A, JAMALI F. Extent of renal effect of cyclo-oxygenase-2-selective inhibitors is pharmacokinetic dependent. *Clin Exp Pharmacol Physiol*. 2006; 33:917-924
- 17) PORTNEY LG, WATKINS MP. 3 ed. Norwalk, CN: Appleton & Lange, 2009.
- 18) DEMIRCAN B, ÇELİK G, SÜLEYMAN H, AKÇAY F. Effects of indomethacin, celecoxib and meloxicam on glutathione, malondialdehyde and myeloperoxidase in rat gastric tissue. *Pain Clinic* 2005; 17:383-388.
- 19) KOCKAYA EA, SELMANOĞLU G, KISMET K, AKAY MT. Pathological and biochemical effects of therapeutic and supratherapeutic doses of celecoxib in Wistar albino male rats. *Drug Chem Toxicol* 2010; 33: 410-414.
- 20) MURRELL DE, RAHMASARI Y, DENHAM JW, PANUS PC, HARIRFOROOSH S. Celecoxib or diclofenac hepatic status in the presence or absence of rebamipide. *Eur Rev Med Pharmacol Sci* 2015; 19: 3318-3325.
- 21) MURRELL DE, DENHAM JW, HARIRFOROOSH S. Histopathology and oxidative stress analysis of concomitant misoprostol and celecoxib administration. *J Toxicol Pathol* 2015; 28: 165-170.

- 22) BATU OS, EROL K. The effects of some nonsteroidal anti-inflammatory drugs on experimental induced gastric ulcers in rats. *Inflammopharmacology* 2007; 15: 260-265.
- 23) SIGTHORSSON G, SIMPSON RJ, WALLEY M, ANTHONY A, FOSTER R, HOTZ-BEHOFSTITZ C, PALIZBAN A, POMBO J, WATTS J, MORHAM SG, BJARNASON I. COX-1 and 2, intestinal integrity, and pathogenesis of nonsteroidal anti-inflammatory drug enteropathy in mice. *Gastroenterology* 2002; 122: 1913-1923.
- 24) HA ES, CHOO GH, BAEK IH, KIM MS. Formulation, characterization, and in vivo evaluation of celecoxib-PVP solid dispersion nanoparticles using supercritical antisolvent process. *Molecules* 2014; 19: 20325-20339.
- 25) MORGEN M, BLOOM C, BEYERINCK R, BELLO A, SONG W, WILKINSON K, STEENWYK R, SHAMBLIN S. Polymeric nanoparticles for increased oral bioavailability and rapid absorption using celecoxib as a model of a low-solubility, high-permeability drug. *Pharm Res* 2012; 29: 427-440